Thermochimica Acta 543 (2012) 9–17

Thermochimica Acta

journal homepage: www.elsevier.com/locate/tca

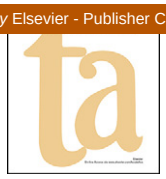

Simultaneous DSC-FTIR spectroscopy: Comparison of cross-linking kinetics of an epoxy/amine resin system

Surya D. Pandita, Liwei Wang, Ramani S. Mahendran, Venkata R. Machavaram, Muhammad S. Irfan, Dee Harris, Gerard F. Fernando *

Sensors and Composites Group, School of Metallurgy and Materials, University of Birmingham, Edgbaston, Birmingham B15 2TT, UK

ARTICLE INFO

Article history:
Received 17 October 2011
Received in revised form 18 April 2012
Accepted 20 April 2012
Available online 9 May 2012

Keywords:
DSC
FTIR spectroscopy
Thermoset
Cross-linking instrumentation

ABSTRACT

The top-cover of a conventional differential scanning calorimeter (DSC) was modified to accommodate two custom-made fibre-optic probes. The function of the probes was to illuminate the sample and reference compartments of the DSC and to return the reflected light from the DSC pans to a fibre-coupled Fourier transform near-infrared (FTIR) spectrometer. The cross-linking kinetics of a commercially available epoxy/amine resin system were studied using the conventional and modified DSC along with conventional transmission FTIR spectroscopy. The cross-linking kinetics and the activation energies for the epoxy/amine resin system obtained via the conventional DSC and simultaneous DSC/FTIR were similar (60.22–60.97 kJ mol^{-1}). However, the activation energy obtained for the cuvette-based conventional transmission FTIR experiments was found to be lower (54.66 kJ mol^{-1}). This may be attributed to the temperature-control attained within the cuvette holder. The feasibility of using a simple fibre-optic probe to link the DSC to the FTIR spectrometer was demonstrated.

1. Introduction

Analytical techniques such as differential scanning calorimetry and Fourier transform infrared (FTIR) spectroscopy are used extensively to characterise the cross-linking of thermosetting resins [1]. However, a direct comparison or cross-correlation of the data generated using a differential scanning calorimeter (DSC) and an FTIR spectrometer are not straightforward for one or more of the following reasons:

(i) *Measurand*. The DSC measures thermally activated processes such as the heat capacity, melting, crystallisation, glass transition temperature and enthalpy of reactions. The data on the enthalpy of the reaction obtained from the DSC represents the sum of all chemical reactions that take place during cross-linking. In contrast, FTIR spectroscopy is associated with the molecular vibrational characteristics of specific functional groups. Therefore, FTIR spectroscopy can impart quantitative information on the depletion or formation of specified functional groups during the course of the cross-linking reaction.

(ii) *Thermal gradients and temperature control*. The methods used to heat the sample in the DSC and FTIR spectrometer are different. The DSC relies on conductive heating where the metal pans, containing the sample and reference (empty pan) are in intimate contact with the sample holder and furnace. Here, the accuracy of temperature-control is generally ±0.05 °C. In the case of FTIR spectroscopy experiments involving thermosetting resins, a "hot-cell" is used where the resin system is contained between a pair of optically transparent windows, for example, quartz windows. A spacer is used between the optical windows to obtain the required path length. In this instance, the resin system predominantly experiences radiative heating and it is difficult to ensure that the specimen does not experience a thermal gradient. This issue is more significant with near-infrared spectroscopy where longer path-lengths are required when compared to mid-infrared-based characterisation.

(iii) *Mass of the sample*. In addition to the fact that the substrates used to contain the specimens in the two techniques are different, the heat-transfer characteristics for the two experiments are different due to variations in the respective sample masses. FTIR spectroscopy requires specimens of approximately 0.5 g (1 mm path-length cuvette), whereas DSC is restricted to 3–15 mg samples. In the former case, the exothermic nature of the cross-linking reaction can result in significant deviation from the desired isothermal temperature.

(iv) *Substrates*. Experiments involving the DSC are carried out using aluminium, copper or steel pans. However, conventional transmission FTIR spectroscopy generally dictates the need for optically transparent materials such as quartz or sodium chloride. Therefore, the possibility of surface-catalysed reactions on

* Corresponding author.
E-mail address: g.fernando@bham.ac.uk (G.F. Fernando).

0040-6031
http://dx.doi.org/10.1016/j.tca.2012.04.024

the various substrates used in the DSC and FTIR spectroscopy experiments cannot be ruled out.

(v) *Environment and volatility of sample*. The experiments that are carried out on a DSC are generally conducted in a nitrogen atmosphere where the sample is contained in an un-crimped open-top pan; the volatility of the sample can be an issue especially when the cross-linking reactions are conducted at elevated temperatures. Volatility of one or more of the components in the resin system can result in a deviation from the desired stoichiometry.

With reference to the above-mentioned issues, apart from the experimental elegance in being able to conduct multi-parameter characterisation on the same test specimen, there is a strong argument in favour of developing hyphenated analytical techniques to characterise materials under one set of environmental and processing conditions.

The following section presents a brief review of selected papers that developed the background technology to enable hyphenated analytical techniques involving the DSC to be realised. Wendlandt [2] provided an overview of the pioneering contributions made by his group to the design and development of a wide range of thermal analysis techniques.

Magill [3] developed a technique to study the crystallisation of poly(hexamethylene adipamide) by tracking the depolarisation of plane-polarised light. In essence, a hot-stage was used in conjunction with a polarising microscope and a photomultiplier; the photomultiplier was connected to a cathode-ray oscillograph. Wendlandt et al. [4] reported on a technique based on diffuse reflectance spectroscopy to study transitions in cobalt (III) complexes and the dehydration of copper sulphate from ambient to 500 °C. The key components of the instrument were: (i) a sample and a reference compartment where only the sample was heated to the required temperature; (ii) thermocouples to measure the temperature; and (iii) a reflectance attachment that was located over the sample and reference compartments to record the reflected radiation as a function of wavelength and temperature. Haines and Skinner [5,6] integrated a stereo microscope with an in-built light source onto a power-compensated DSC. A CdS detector was positioned on one of the eyepieces to record the reflected light intensity from the sample pan, whilst the thermal properties were recorded via the DSC. The second eyepiece was used to photograph the phase change in the test specimen that was contained in the sample compartment of the DSC. They reported that the integration of the binocular microscope onto the DSC did not have any adverse influence on the performance of the instrument. A range of organic and inorganic substances was used to study the melting, crystallisation and dehydration processes.

The majority of the previous research on linking thermal analysis equipment to a FTIR spectrometer was carried out using heat-flux DSC and a microscope accessory. For example, Mirabella [7,8] used the orifice on the sample compartment of the DSC to facilitate the infrared radiation from a spectrometer to be transmitted through the sample. The samples were generally mounted on an optically transparent medium such as potassium bromide or sodium chloride discs. Due to a poor signal-to-noise ratio, it was necessary to use thicker samples in the reference compartment of the DSC. This meant that the thermal and spectral analyses were carried out on two separate test specimens. This limitation was overcome by Johnson et al. [9], where the spectral interrogation of the specimen in the DSC was carried out in reflection-mode. Examples of other researchers who have utilised the simultaneous DSC/FTIR spectroscopy technique include DeBakker et al. [10], Lin et al. [11] and Ziegler et al. [12]. DeBakker et al. [10] employed near-infrared spectroscopy to study the cross-linking of a commercially available epoxy/amine resin system. They used glass pans to contain the mixed resin system and an external light source was used to illuminate the specimen. The transmitted light was directed to the detector port of an FTIR spectrometer; this approach required a series of collimating lenses to focus, transmit and collect the light.

The introduction of an optical fibre probe into a DSC was demonstrated by Frushour and Sabatelli [13]. They drilled the top-cover of a conventional power-compensated DSC to accommodate a pair of fibre-optic probes over the sample and reference compartments. The fibre-optic probe that was located over the reference compartment of the DSC was not illuminated. The “active” probe consisted of a bifurcated bundle of randomly arranged transmitting and receiving optical fibres. The sensing or distal end of the probe was housed in a brass tube. The intensity of the reflected light from the sample compartment of the DSC was acquired simultaneously with the thermal analyser. These authors reported a discrepancy of 1 °C with regard to the melting point of pure indium when the experiments were carried out on the modified DSC. They attributed this observation to heat loss as a consequence of the removal of the platinum lids that are used with conventional DSCs. The enthalpy of fusion was reported to be unchanged. The heating effect of the light source (800 nm) was investigated and reported to be in the order of 0.15 mW. They termed this technique thermal optical analysis (TOA). Kloosterboer et al. [14] reported on the modification of a power-compensated DSC to enable the photo-irradiation of the sample. This technique was later adapted by Kloosterboer et al. [15] to enable simultaneous photo-DSC and turbidity measurements to study polymerisation-induced phase separation of polymer-dispersed liquid crystals.

Harju et al. [16] removed the chamber of a power-compensated DSC and secured it in the sample compartment of a FT-Raman spectrometer. They demonstrated that simultaneous Raman and DSC data could be obtained to study the phase transitions in ammonium nitrate between 300 and 425 K. Sprunt and Jayasooriya [17] extended this technique by coupling the two instruments via a fibre-optic probe. Other notable research pertaining to the development and demonstration of hyphenated analytical techniques include the work of Koberstein and Russell [18], Dumitrescu et al. [19], Degamber et al. [20] and Degamber and Fernando [21].

In the current paper, the simultaneous DSC/FTIR technique developed by Degamber et al. [20] was used to study the cross-linking kinetics of an epoxy/amine thermosetting resin system. Experiments were conducted using the original DSC top-cover and one where it was modified to accommodate the non-contact fibre-optic probes. Data from the conventional and modified DSC are compared with the transmission/reflection FTIR data obtained from the fibre-optic probes. The resin system was also characterised using conventional transmission FTIR spectroscopy where a 1 mm path-length cuvette was used in conjunction with a temperature-controlled cuvette holder.

2. Experimental

2.1. Epoxy/amine resin systems

The epoxy/amine resin system used in the current work was Araldite LY3505/XB3403 (Huntsman Advanced Materials, UK). The materials were used as-supplied without further purification. A fresh batch of the LY3505/XB3403 resin system was prepared just prior to the commencement of each experiment. The resin system was mixed thoroughly in the stoichiometric ratio of 100:35 (LY3505:XB3403) by weight. This was followed by degassing in a vacuum chamber for 15 min. The resin system was cross-linked isothermally at 40, 50, 60 and 70 °C.

2.2. Conventional FTIR spectroscopy

A Bruker MATRIX^{TM}-F duplex FT-NIR spectrometer (Bruker Optics Ltd., UK) was employed for monitoring the cross-linking of the epoxy/amine resin system. The spectrometer was set to operate in the near-infrared region from 11,000 to 4000 cm^{-1}. Spectra were collected at a resolution of 4 cm^{-1} over 64 scans. The mixed resin was injected, via a syringe, into a de-mountable (open-end) optical glass cell with a path-length of 1 mm (Starna, UK). The cell was housed in a CUV-TLC-50F temperature-regulated cuvette holder (Ocean Optics Inc., USA). The cuvette holder had two optical ports accommodating a pair of sub-miniature adapter (SMA) connectors with integrated collimating lenses. With reference to the conventional FTIR spectroscopy transmission experiments, two low-OH optical fibre probes (Ocean Optics Inc., USA) were used to deliver and collect the light to and from the resin contained in the cuvette.

2.3. Conventional DSC

The conventional DSC experiments were conducted on a Diamond DSC (PerkinElmer Inc., UK). The instrument was calibrated with pure indium and tin prior to use. The sample and reference compartments of the calorimeter were purged with nitrogen gas at a flow of 30 cm^3/min. The resin and hardener mixture was prepared just prior to use, and approximately 15 mg was placed in an open (uncrimped) aluminium pan. In the case of the dynamic scans, these were performed from 30 to 250 °C at a heating rate of 5 K/min. With reference to the isothermal experiments, the sample was placed in the DSC chamber which was pre-set at 30 °C and then ramped at 40 K/min to the desired cross-linking temperature of: 40, 50, 60 or 70 °C.

2.4. Simultaneous DSC/FTIRS

With reference to Fig. 1, the top-cover of a conventional PerkinElmer Diamond DSC was removed and replaced with a custom-modified top-cover from a PerkinElmer DSC-7 calorimeter. The gas exhaust ports on the top-cover, located above the sample and reference compartments, were drilled out to accommodate two arms of an optical fibre probe. The two arms of the probe were secured to vertical translation stages to enable the distance between the ends of the probes and the sample and reference pans to be controlled as desired. A schematic illustration of the fibre-optic probe assembly and the DSC is shown in Fig. 1(i); Fig. 1(ii) shows a cut-out side view of the fibre-optic probes and the DSC furnace compartment.

With reference to Fig. 1, the two arms of the probes were held using conventional translation stages and this assembly was secured above the sample and reference compartments of the DSC. Each arm of the probe that was integrated into the DSC contained around 150 low-OH 105/125 μm silica optical fibres. These optical fibres were potted in individual silica tubes and polished. The three distal-ends of the probe were potted into SMA connectors and polished using conventional procedures; the arm that was connected to the light source consisted of around 150 fibres and each of the other two arms, contained approximately 75 optical fibres, were connected to two detector-ports of the FTIR spectrometer.

In the case of the simultaneous DSC/FTIR experiments, the spectrometer and calorimeter were operated as described previously.

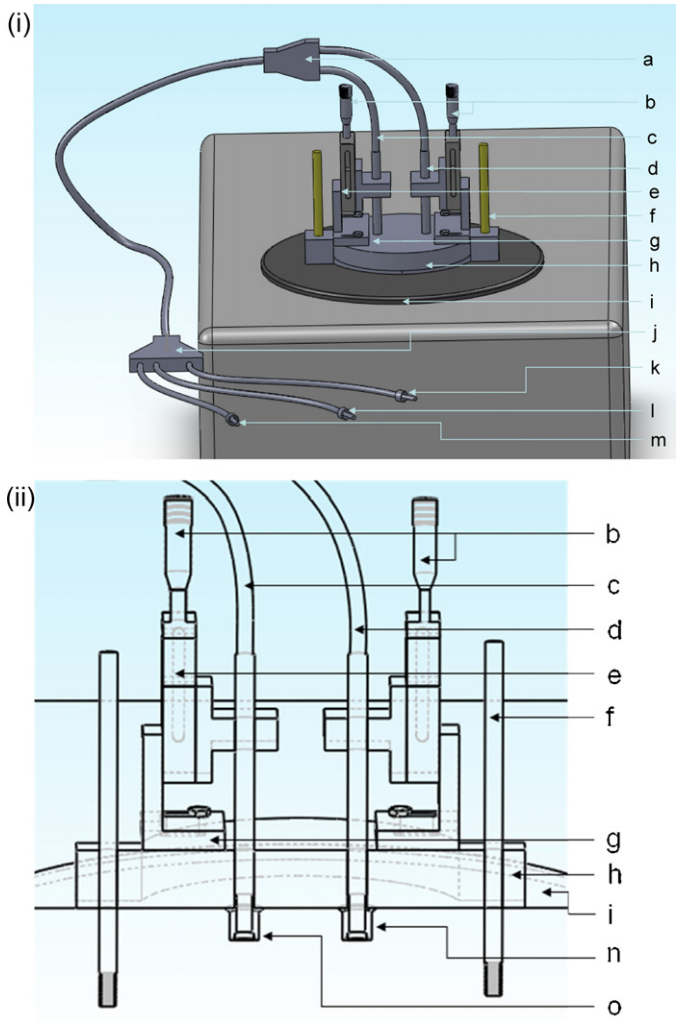

Fig. 1. (i) A schematic illustration of the custom-modified top-cover of the Diamond DSC and the fibre-optic probe assembly. (ii) A side-on view of fibre-optic probes and the furnace compartments of the DSC. a: Housing for the 1*2 fibre-optic probe assembly; b: translation stages to raise or lower the fibre-optic probes; c: fibre-optic probe positioned over the sample compartment; d: fibre-optic probe located over the reference compartment; e: support fixture for the translation stage; f: support fixture to enable the top cover of the DSC to be located into position; g: attachment point between the DSC cover and the translation stage fixture; h: DSC-7 cover (top-lid); i: base plate of the Diamond DSC; j: 3*1 housing for the fibre-optic probe; k: connector for the light source from the FTIR spectrometer; l: SMA connector for the detector (reflected light from the sample pan of the DSC); m: SMA connector for the detector (reflected light from the reference pan of the DSC); and n and o: cut-out side view showing the relative positions of the DSC chambers (sample and reference compartments) and the fibre-optic probe assembly.

3. Results and discussion

3.1. Conventional DSC and simultaneous DSC/FTIR

With reference to the reactive functional groups that are present in the resin system, the extent of conversion (α) is defined as:

$$\alpha = \frac{\Delta H_t}{\Delta H_{dyn}} \quad (1)$$

where ΔH_t is the cumulative enthalpy of the reaction at time t, ΔH_{dyn} is the total heat of the curing reaction determined by a

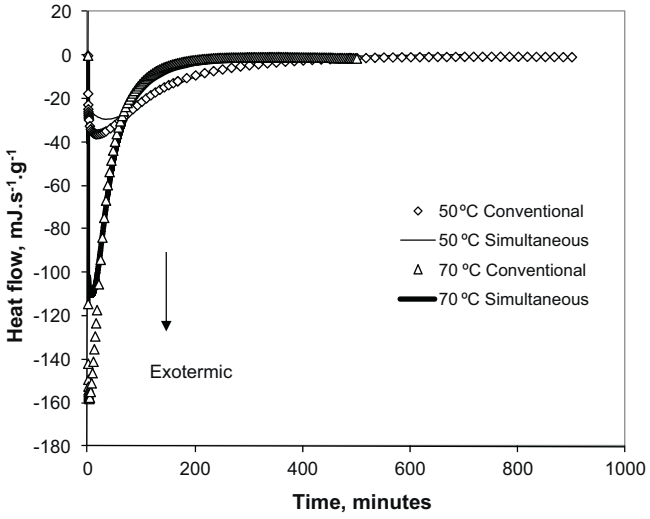

Fig. 2. Thermal analysis data obtained using the conventional DSC and the simultaneous DSC/FTIR techniques, conducted isothermally at 50 and 70 °C.

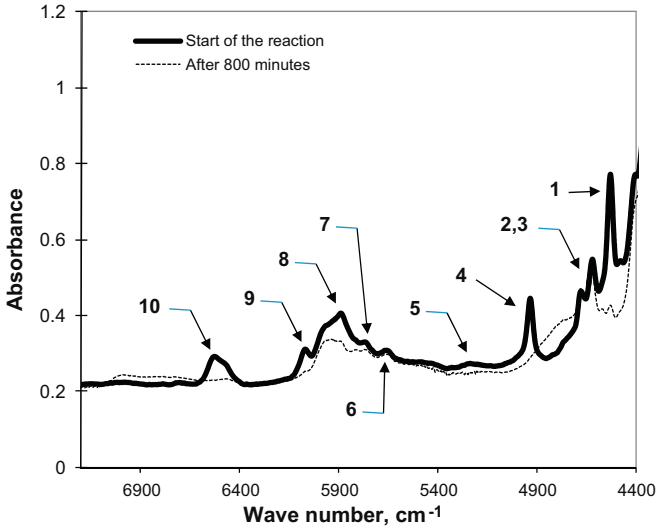

Fig. 3. Absorbance spectra for the LY3505/XB3403 resin system at the start of the cross-linking reaction and after 800 min.

non-isothermal (dynamic) scan. The cumulative enthalpy of the reaction can be calculated as follows:

$$\Delta H_t = \int_0^t \frac{dH}{dt} dt \quad (2)$$

where dH/dt is the heat flow obtained from the DSC measurements.

Fig. 2 shows the cross-linking or cure data obtained using the conventional and simultaneous DSC techniques, conducted isothermally at 50 and 70 °C. Here, the heat flow was normalised to the mass of the sample. At the beginning of the cross-linking reaction, the enthalpy obtained via the conventional DSC is slightly higher than that observed for the simultaneous DSC/FTIR setup. This discrepancy may be due to the time taken to attain thermal equilibrium within the DSC chamber when the silica-based fibre-optic probes are present. It is worth noting that the calorimeter was calibrated with pure indium and tin for situations with and without the fibre-optic probe. After approximately 10 min at the isothermal cross-linking temperature, the outputs from the conventional and simultaneous DSC/FTIR experiments were similar.

3.2. Monitoring the epoxy functional group during cross-linking using FTIR spectroscopy

The reflected light from the fibre-optic probe that was located over the sample compartment of the DSC/FTIR setup was directed to the fibre-coupled FT-NIR spectrometer. The absorbance of the epoxy functional group was tracked during the cross-linking reactions. Typical spectra for the LY3505/XB3403 epoxy/amine resin system at the start of the reaction and after 800 min are illustrated in Fig. 3. The peak assignments for the absorbance spectra shown in Fig. 3 are summarised in Table 1.

An expanded view of Fig. 3 is presented in Fig. 4 where, as expected, the epoxy peak at 4530 cm^{-1} is seen to decrease as a function of time during the cross-linking process. After approximately 50% of the conversion of the epoxy functional group, the emergence of a small peak at 4564 cm^{-1} is apparent. The prominence of this unassigned peak became more evident with the depletion of the epoxy peak at 4530 cm^{-1}; it is speculated that the peak may be due to a combination band of C—H stretching vibration of the aromatic ring and aromatic C=C conjugated stretching vibration [23]. Previous researchers have also noted the presence of this unassigned peak [24–26]. The contribution of this unassigned peak to the epoxy functional group absorbance was assessed via a deconvolution routine.

Fig. 5 shows the deconvoluted epoxy spectra obtained using the Fourier self-deconvolution (FSD) routine contained in the Bruker OPUS software. A Lorentzian line shape with a bandwidth of 5 cm^{-1} and a resolution enhancement of 1.5 were selected for the FSD manipulation. As seen in Fig. 5, the deconvolution routine enabled the epoxy and the unknown peaks to be resolved. If deconvolution is not performed on the absorbance spectra shown in Fig. 4, the contribution of the unassigned peak area to that of the epoxy peak areas was estimated to be less than 5% of the initial epoxy peak. Analysis of the deconvoluted area for the unassigned peak indicated that it remained constant throughout the reaction. Therefore, when the two peaks are not deconvoluted, there is justification in subtracting the contribution of the unassigned peak area from the epoxy peak area at 4530 cm^{-1}.

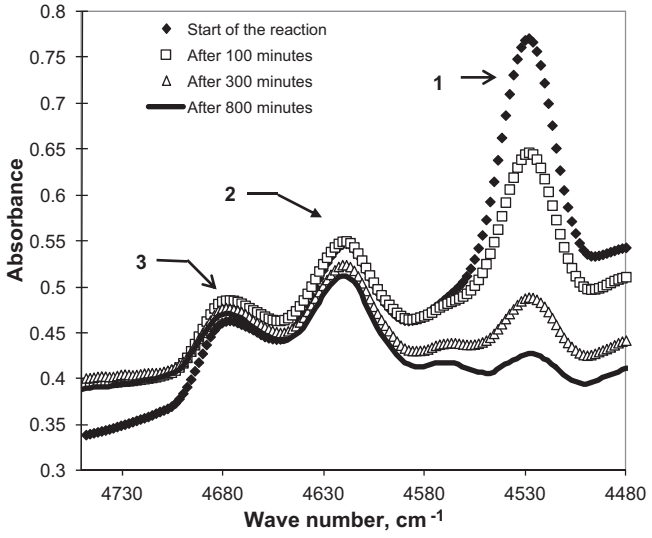

Fig. 4. Absorbance spectra for the LY3505/XB3403 resin system cross-linked at 50 °C at the start of the cross-linking reaction and after 100, 300 and 800 min.

Table 1
Peak assignments for the epoxy/amine resin system [22,25,28].

Peak label	Wave number (cm^{-1})	Peak assignment
1	4530	Epoxy combination band (C—H stretching and epoxy ring breathing)
2, 3	4620, 4677	Aromatic combination band (C—H stretching)
4	4935	Primary amine combination band (N—H stretching and bending)
5	5249	—OH due to moisture (O—H asymmetric stretching and bending)
6	5668	Aliphatic, terminal R—CH_3 overtone (stretching)
7	5767	Methyl 1st overtone (C—H stretching)
8	5889	Combination band of epoxy and primary amine overtones
9	6067	Terminal epoxy 1st overtone (C—H stretching)
10	6635	Primary and secondary amine combination band (overtones of N—H stretching)

The extent of reaction or conversion (α) of the epoxy functional group is generally calculated by referencing it to an inert peak [27]:

$$\alpha_{\text{epoxy},t} = 1 - \left(\frac{(A_{\text{epoxy},4530}/A_{\text{reference},4620})_t}{(A_{\text{epoxy},4530}/A_{\text{reference},4620})_{t=0}} \right) \quad (3)$$

where A_{epoxy} and $A_{\text{reference}}$ are the areas of the epoxy and reference peaks respectively, t represents the time during the cross-linking reaction and $t = 0$ represents the start of the reaction. The aromatic C—H combination band at 4620 cm^{-1} is an inert peak as it does not take part in the cross-linking reaction and hence this peak area was used to normalise that of the epoxy absorbance peak area (centred at 4530 cm^{-1}).

Eq. (3) can also be applied to calculate the conversion of the primary amine at 4935 cm^{-1}. As mentioned previously, the inert aromatic C—H peak at 4620 cm^{-1} was also used to normalise the primary amine peak area:

$$\beta_{\text{PA},t} = \frac{(A_{\text{PA},4935}/A_{\text{reference},4620})_t}{(A_{\text{PA},4935}/A_{\text{reference},4620})_{t=0}} \quad (4)$$

where PA refers to the primary amine absorption band at 4935 cm^{-1} and β_{PA} is the normalisation of the primary amine. Fig. 6(i) shows the depletion of the primary amine peak at specified intervals during the cross-linking reaction. During this process, the primary amine is converted to a secondary which in turn is converted to a tertiary amine. The absorbance band for the secondary amine functional group appears between 6600 and 6400 cm^{-1} as an overlapped band with the primary amine and is shown in Fig. 6(ii).

The concentration of the secondary amine can be determined by subtracting the primary amine group concentration from the combined peak, as detailed in Eqs. (5) and (6).

$$\Delta A_{6600-6400,t} = (E_1[\text{PA}]_t + E_2[\text{SA}]_t)l \quad (5)$$

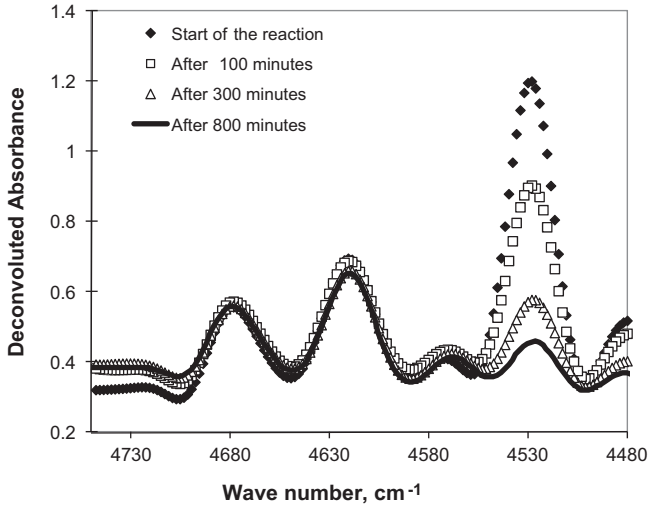

Fig. 5. Deconvoluted spectra of Fig. 4 obtained using Fourier self-deconvolution.

$$[\text{SA}]_t = \frac{[\Delta A_{6600-6400,t} - E_1 \cdot l[\text{PA}]_t]}{E_2 \cdot l} \quad (6)$$

where $\Delta A_{6600-6400,t}$ is the peak area between 6600 cm^{-1} and 6400 cm^{-1} at time t. E_1 and E_2 are the molar absorptivities of the primary and secondary amines respectively, and $[\text{SA}]_t$ is the concentration of secondary amine at time t. l is the optical path length.

For a stoichiometric bi-functional epoxy and amine system, the concentrations of the secondary and tertiary amine groups (A_2 and

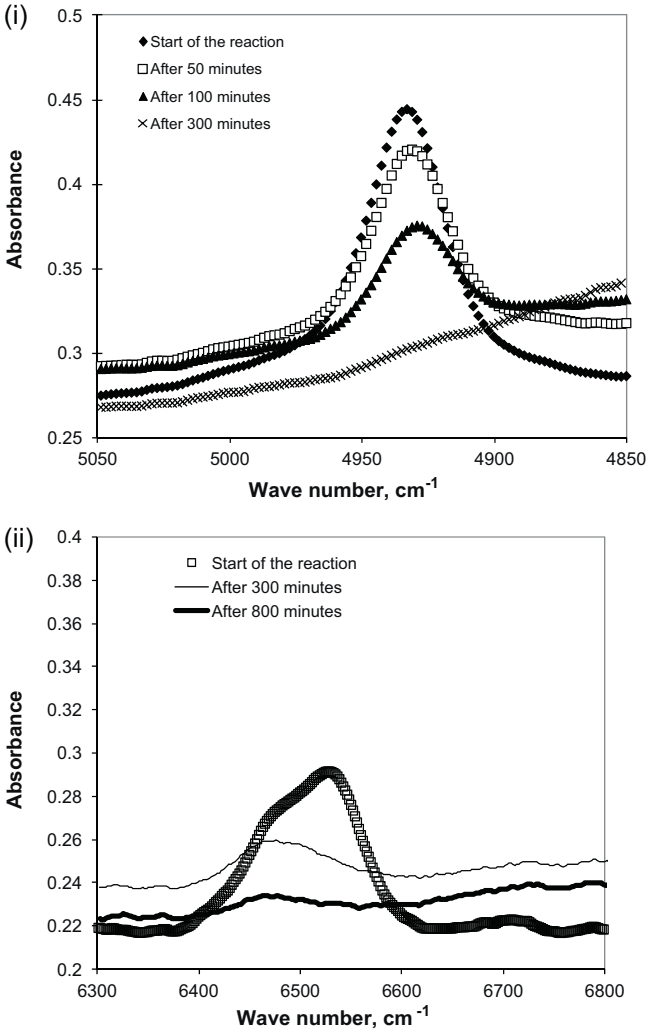

Fig. 6. Absorbance spectra of the LY3505/XB3403 resin system when cross-linked isothermally at 50 °C using the simultaneous DSC/FTIR technique for: (i) the amine peak at the start of the cross-linking reaction and after 50, 100 and 300 min; and (ii) the combined peak of primary and secondary amines at the start of the cross-linking reaction and after 300 and 800 min.

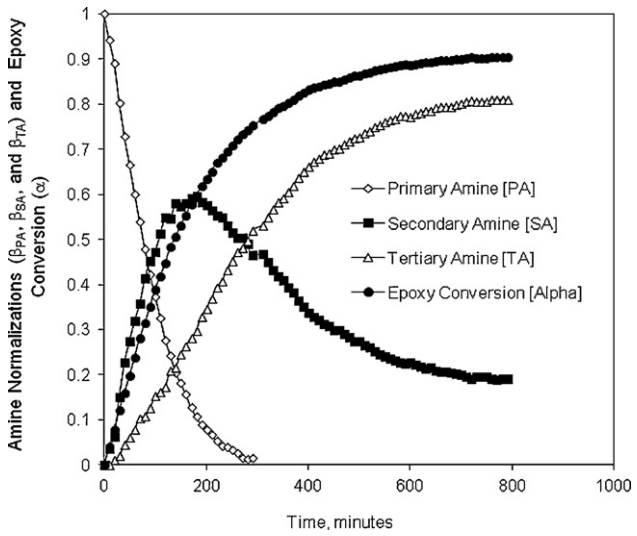

Fig. 7. Conversion data for the epoxy and the normalisation data of the primary, secondary and tertiary amines when the LY3505/XB3403 resin system is cross-linked isothermally at 50 °C.

A_3 respectively) can be calculated using a mass balance approach [33]:

$$A_2 = E_0 \cdot ((1 - \beta_{PA,t})B - \alpha_t) \quad (7)$$

$$A_3 = E_0 \cdot \left(\alpha_t - \frac{B}{2}(1 - \beta_{PA,t})\right) \quad (8)$$

where

$$B = \frac{2A_{1,0}}{E_0} \quad (9)$$

Rearranging Eqs. (7) and (8):

$$\frac{A_2}{A_{1,0}} = \beta_{SA,t} = 2\left(1 - \beta_{PA,t} - \frac{\alpha_t}{B}\right) \quad (10)$$

$$\frac{A_3}{A_{1,0}} = \beta_{TA,t} = \frac{2}{B}\alpha_t + \beta_{PA,t} - 1 \quad (11)$$

where $\beta_{SA,t}$ and $\beta_{TA,t}$ refer to the normalisations of the secondary and tertiary amine groups at time t respectively. E_0 is the initial concentration of the epoxy and $\beta_{PA,t}$ is the normalisation of the primary amine at time t. B is the ratio of primary amine to epoxy concentration at the start of the reaction; for a stoichiometric mixture, the value of B is equal to 1. α_t refers to the extent of conversion or conversion reaction at time t. Fig. 7 shows the conversion data for the epoxy and the primary, secondary and tertiary amines during cross-linking at 50 °C.

3.3. Cross-linking kinetics

The cure kinetics of thermosetting polymers have been studied widely and a variety of kinetic models have been proposed to relate the rate of the chemical reaction to the processing time, temperature, and the extent of the reaction (conversion) [28–32]. In the current study, the "autocatalytic model" [32] was used to model the cross-linking data from the conventional DSC and the simultaneous DSC/FTIR. The autocatalytic model is described by Eq. (12):

$$\frac{d\alpha}{dt} = k\alpha^m \cdot (1 - \alpha)^n \quad (12)$$

where k is the rate constant, α is the conversion reaction, and m and n represent the reaction orders. In subsequent graphs, the best fit to the data were obtained by using $m = 0.35$ and $n = 1.65$.

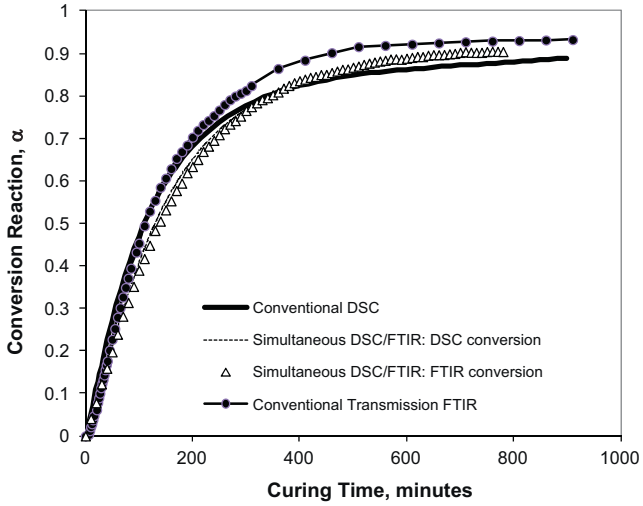

Fig. 8. Conversion of the epoxy functional group studied by conventional transmission FTIR spectroscopy, simultaneous DSC/FTIR (conversion based on the DSC and FTIR) and conventional DSC plotted against cure time at 50 °C.

Figs. 8 and 9 show the degree of conversion for the epoxy functional group where the cross-linking reactions were carried out at 50 and 70 °C respectively. The data were generated using the conventional DSC, modified DSC (DSC/FTIR), conventional FTIR spectroscopy (1 mm path length cuvette) and near-infrared spectroscopy via the fibre-optic probe on the simultaneous DSC/FTIR. With reference to Figs. 8 and 9, the following observations can be made:

(i) The degree of conversion obtained using the simultaneous DSC/FTIR technique (epoxy conversion via reflection FTIR spectroscopy and thermal analysis via the modified DSC) show an excellent correlation; this was observed for the four temperatures investigated in this study. The FTIR spectra obtained are best described as transmission/reflection; this is because the infrared light is transmitted through the resin and is reflected off the aluminium pan. Since the absorbance data are normalised to the inert C—H absorbance band, path-length differences are taken into account. It can be concluded that if the temperature within the processing equipment can be

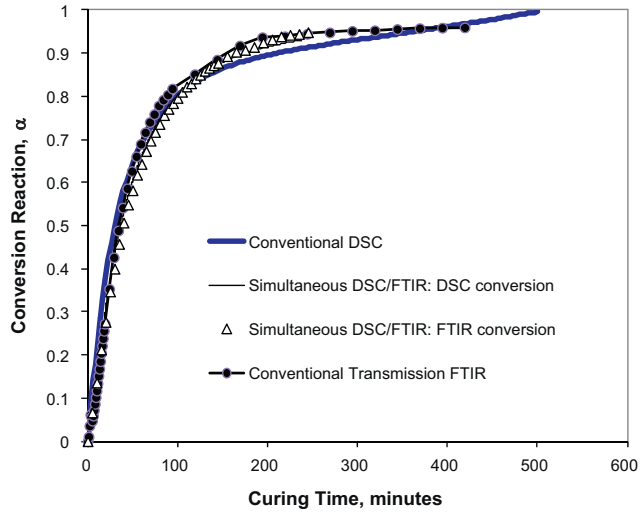

Fig. 9. Conversion of the epoxy functional group studied by the simultaneous DSC/FTIR technique (conversion based on the DSC and FTIR) and conventional transmission FTIR spectroscopy and conventional DSC plotted against cure time at 70 °C.

assured to be uniform, the cross-linking kinetics from FTIR spectroscopy and thermal analysis should be similar when the same sample is analysed; this is the case with simultaneous DSC/FTIR spectroscopy used in the current study.

(ii) On comparing the datasets for the conventional DSC and the simultaneous DSC/FTIR, a common trend is observed where the rate of conversion is higher for the conventional DSC up to approximately 55% conversion; after this point, the rate of conversion is seen to slow down significantly. Interestingly, the extent of the reaction for the conventional DSC is seen to be lower than that observed for the simultaneous DSC/FTIR combination and conventional transmission FTIR spectroscopy; the observed discrepancies were lower at the higher isothermal temperature. These trends are also reflected in the rate constants summarised in Table 2 for the resin system for the four different analytical techniques.

(iii) The observed differences between the conversion data for the conventional and simultaneous DSC may be attributed to the calibration procedures used. The calibrations of the conventional and simultaneous DSC/FTIR were carried out (using pure indium and tin) with and without the fibre-optic probes respectively. The presence of the fibre-optic probes does influence the thermal environment within the DSC chamber but it was assumed that the calibration procedures would compensate for this. However, the thermal conductivity of the resin system is significantly lower than that of the calibration medium (indium and tin) and it is possible that the observed differences between the conventional and simultaneous DSC/FTIR could be reduced using organic reference standards. This will be investigated and reported in due course. Nevertheless, the cross-linking kinetics and the activation energies derived for the epoxy/amine resin system yield similar results. This demonstrates that if the temperature regime is identical, the rates of depletion of the epoxy and amine functional groups will be similar. Moreover, since the analyses were performed on the same sample, the kinetics from the simultaneous DSC/FTIR and FTIR spectroscopy will be similar.

With reference to Eq. (12), the temperature dependency of the rate constant is given by the Arrhenius relationship:

$$k = A \cdot \exp\left(\frac{-E}{RT}\right) \tag{13}$$

where A is a pre-exponential factor, E is the activation energy, R is the universal gas constant, and T is the temperature. A summary of the respective activation energies for the resin system when using the four different analytical techniques is presented in Table 2. Whilst the activation energies for the simultaneous DSC/FTIR and conventional DSC are similar (60.22–60.97 kJ mol^{-1}), the conventional transmission FTIR spectroscopy yields a value of 54.66 kJ mol^{-1}. Given the fact that the resin system used in these experiments was the same, the following reason may have contributed to the observed lower value for the activation energy associated with the conventional transmission FTIR spectroscopy experiments. The relative masses of the samples used in the DSC and conventional FTIR spectroscopy were 15 mg and 0.5 g respectively. Since the cross-linking reactions are exothermic, efficient temperature management is important. It is therefore possible that the isothermal conditions may not have been maintained in the cuvette holder; this may explain the higher conversion rate and extent of conversion for the cuvette-based experiments. In the case of the power-compensated DSC, the smaller sample mass and the intimate contact between the sample, the sample holder (aluminium pan) and the furnace facilitates efficient temperature regulation.

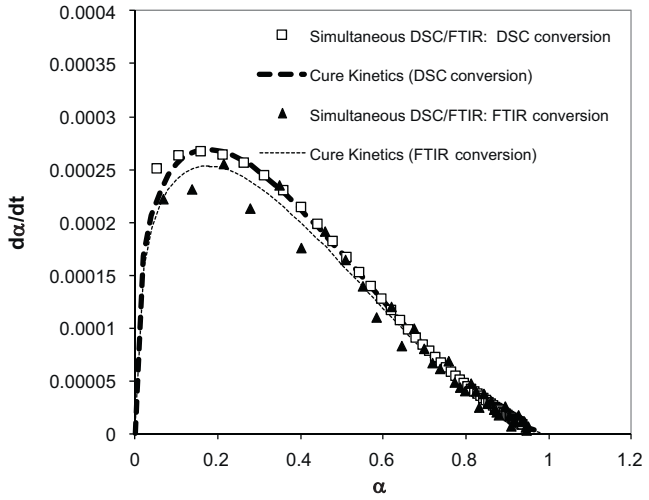

Fig. 10. Cure rate plotted against conversion: simultaneous DSC/FTIR, conventional DSC and conventional transmission FTIR spectroscopy at 70 °C.

The phenomenological autocatalytic model was used to study the cure kinetics of the epoxy measured by conventional DSC and simultaneous DSC/FTIR. Figs. 10 and 11 show the cure rate of the epoxy/amine system investigated using this model. Matlab® software was used to fit the cure data. Table 2 lists the reaction constant calculated with the autocatalytic model for conventional DSC and simultaneous DSC/FTIR.

Fig. 12 shows the natural logarithm of the reaction constants plotted against reciprocal temperature ($1/T$). Error bars of 5% were added to the average reaction constants obtained from the simultaneous FTIR to show that the reaction constants measured using both conventional DSC and simultaneous DSC/FTIR were not significantly different. With reference to Table 2, the activation energy of the cure reaction for the conventional DSC (60 kJ mol^{-1}) and simultaneous DSC/FTIR (61 kJ mol^{-1}) are similar.

The integration of the autocatalytic model (Eq. (12)), as shown in Eq. (14), under isothermal conditions and with $m + n = 2$, leads to Eq. (15). Fig. 13 shows the conversions from the integration of the autocatalytic model against the curing time for the conventional DSC and simultaneous DSC/FTIR datasets. In Eqs. (14) and (15), the reaction orders "m" and "n" are 0.35 and 1.65 respectively. The reaction constant of the autocatalytic model is the averaged reaction

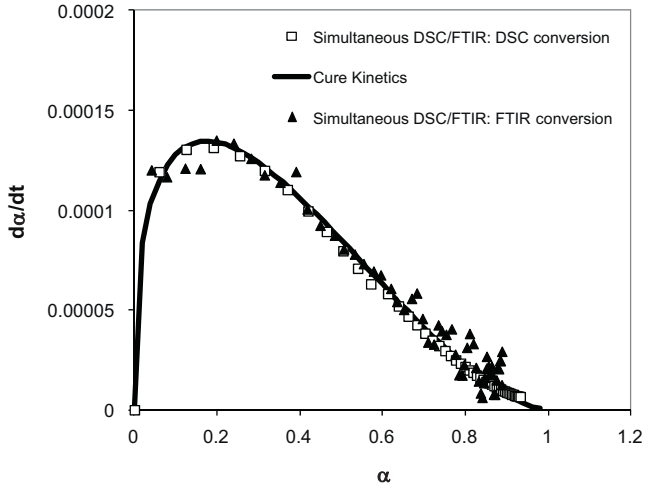

Fig. 11. Cure rate plotted against conversion: simultaneous DSC/FTIR: FTIR conversion of the epoxy group and DSC/FTIR: DSC conversion of the epoxy group at 60 °C.

Table 2
Rate constants obtained and activation energies using the autocatalytic model ($m = 0.35$, $n = 1.65$).

Temperature (°C)	Simultaneous DSC/FTIR				Conventional DSC		Conventional transmission FTIR	
	FTIR		DSC		k	$\ln k$	k	$\ln k$
	k	$\ln k$	k	$\ln k$				
40	8.4E−05	−9.38469	0.000088	−9.33817	0.000105	−9.16155	0.00011	−9.11503
50	0.00017	−8.67971	0.00019	−8.56849	0.00022	−8.42188	0.00024	−8.33487
60	0.00034	−7.98656	0.00035	−7.95758	0.00045	−7.70626	0.00042	−7.77526
70	0.00065	−7.33854	0.00068	−7.29342	0.0008	−7.1309	0.0007	−7.26443
Activation energy (kJ mol^{-1})	60.97		60.22		60.82		54.66	

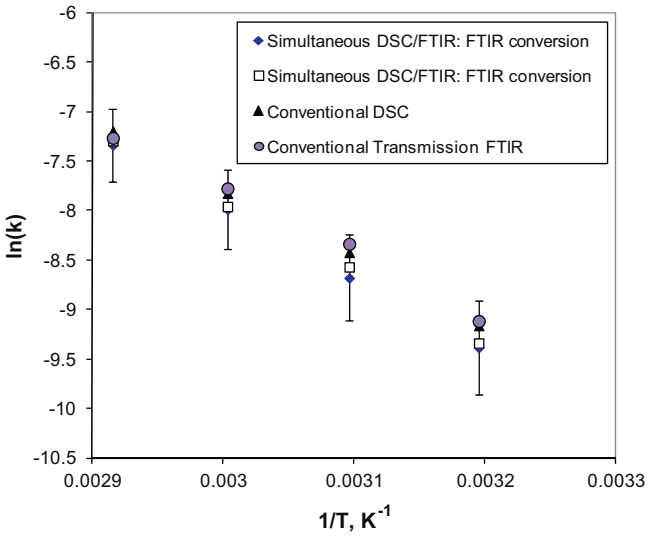

Fig. 12. Arrhenius plot for the LY3505/XB3403 epoxy/amine resin system.

constants of the conventional DSC and the simultaneous DSC/FTIR. All the conversion data obtained from the simultaneous DSC/FTIR fall within the autocatalytic conversion range, whose error bars were 5% of their value. This indicates that the cross-linking kinetic data obtained using the simultaneous DSC/FTIR technique can be described by the autocatalytic model.

$$\int \frac{d\alpha}{\alpha^m(1-\alpha)^n} = \int k \cdot dt \tag{14}$$

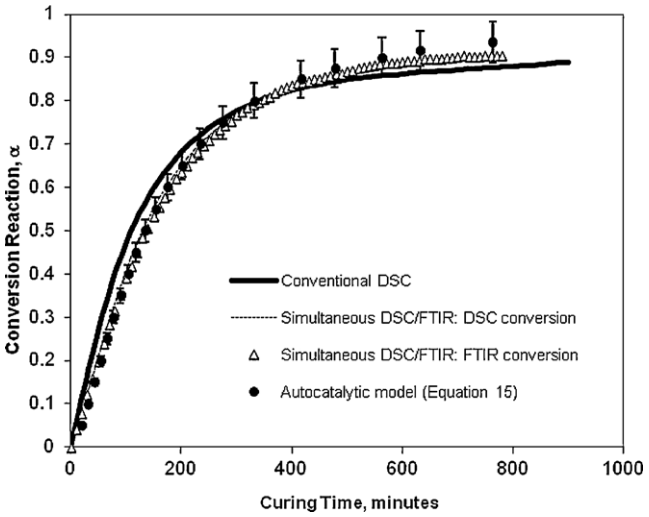

Fig. 13. Conversions calculated from the autocatalytic model ($m = 0.35$ and $n = 1.65$) compared to conversions obtained from the conventional DSC and simultaneous DSC/FTIR for cross-linking at 50 °C.

$$t = \frac{1}{k}\frac{1}{n-1}\left(\frac{\alpha}{1-\alpha}\right)^{n-1} \tag{15}$$

4. Conclusions

This study has demonstrated that a conventional DSC can be adapted to enable simultaneous spectral and thermal information to be extracted during the cross-linking of a thermosetting resin. The cross-linking kinetics of a commercially available epoxy/amine resin system were studied and it was shown that the activation energies for conventional and modified DSC were similar. An excellent correlation was observed between the FTIR spectroscopic data and that obtained from the modified DSC. The cross-linking kinetic data obtained from the cuvette-based conventional transmission FTIR spectroscopy was 54.66 kJ mol^{-1} whereas those obtained from the conventional DSC, simultaneous DSC and reflection FTIR spectroscopy were 60.82, 60.22 and 60.97 kJ mol^{-1} respectively. The discrepancy with the cuvette-based experiment has been attributed to non-isothermal conditions within the cuvette holder. In other words, the temperature within the cuvette holder was raised due to the exothermic nature of the thermosetting resin used in this study.

Acknowledgements

The authors wish to acknowledge financial support from the EPSRC (TS/G000387/1) and the Technology Strategy Board, Projects AB134K, AB135A and BD072K. The support given by the industrial partners (Huntsman Advanced Materials, Pultrex, PPG, CTM, Mould Life, Bruker Optics, Luxfer Gas Cylinders, Halyard, and Huntsman Polyurethanes) is duly acknowledged. GF acknowledges the financial support provided by the Royal Society. The authors wish to acknowledge the technical assistance provided by Professor Brian Ralph, Professor Banshi Gupta, Mark Paget, Seb Ballard, Colin Barrow and Frank Biddlestone. The authors wish to thank Paul Clarke of PETA Solutions for providing the top-cover of the DSC and technical support.

References

[1] G.F. Fernando, B. Degamber, Process monitoring of fibre reinforced composites using optical fibre sensors, Int. Mater. Rev. 51 (2006) 65–106.
[2] W.W. Wendlandt, The development of thermal analysis instrumentation 1955–1985, Thermochim. Acta 100 (1986) 1–22.
[3] J.H. Magill, A new method for following rapid rates of crystallization. 1. Poly(hexamethylene adipamide), Polymer 2 (1961) 221–233.
[4] W.W. Wendlandt, J.P. Smith, P.H. Franke, High temperature diffuse reflectance spectroscopy, Anal. Chem. 35 (1963) 105–107.
[5] P.J. Haines, G.A. Skinner, Simultaneous differential scanning calorimetry and reflected light-intensity measurement, Thermochim. Acta 59 (1982) 343–359.
[6] P.J. Haines, G.A. Skinner, Simultaneous differential scanning calorimetry and reflected light-intensity measurements in polymer studies, Thermochim. Acta 134 (1988) 201–206.
[7] F.M. Mirabella, Simultaneous differential scanning calorimetry (DSC) and infrared-spectroscopy using an infrared microsampling accessory (IRMA) and FT-IR, Appl. Spectrosc. 40 (1986) 417–420.
[8] F.M. Mirabella, Simultaneous differential scanning calorimetry and infrared-spectroscopy, Adv. Chem. Ser. 227 (1990) 357–375.

[9] D.J. Johnson, D.A.C. Compton, P.L. Canale, Applications of simultaneous DSC FTIR analysis, Thermochim. Acta 195 (1992) 5–20.
[10] C.J. DeBakker, N.A. St John, G.A. George, Simultaneous differential scanning calorimetry and near-infra-red analysis of the curing of tetraglycidyl-diaminodiphenylmethane with diaminodiphenylsulphone, Polymer 34 (1993) 716–725.
[11] S.Y. Lin, C.M. Liao, G.H. Hsiue, A reflectance FTIR/DSC microspectroscopic study of the nonisothermal kinetics of anhydride formation in eudragit 1–100 films, Polym. Degrad. Stab. 47 (1995) 299–303.
[12] B. Ziegler, K. Herzog, R. Salzer, In situ investigations of thermal-processes in polymers by simultaneous differential scanning calorimetry and infrared-spectroscopy, Mol. Struct. 348 (1995) 457–460.
[13] B.G. Frushour, D.C. Sabatelli, Simultaneous measurement of light transmission and heat-flow in a modified differential scanning calorimeter, J. Appl. Polym. Sci. 36 (1988) 1453–1465.
[14] J.G. Kloosterboer, G.M.M. Vandehei, R.G. Gossink, G.C.M. Dorant, The effects of volume relaxation and thermal mobilization of trapped radicals on the final conversion of photopolymerized diacrylates, Polym. Commun. 25 (1984) 322–325.
[15] J.G. Kloosterboer, C. Serbutoviez, F.J. Touwslager, Monitoring of polymerization -induced phase separation by simultaneous photo-DSC/turbidity measurements, Polymer 37 (1996) 5937–5942.
[16] M.E.E. Harju, J. Valkonen, Simultaneous application of Fourier-transform Raman-spectroscopy and differential scanning colorimetry for the in situ investigation of phase-transitions in condensed matter, Spectrochim. Acta A: Mol. Biomol. Spectrosc. 47 (1991) 1395–1398.
[17] J.C. Sprunt, U.A. Jayasooriya, Simultaneous FT-Raman differential scanning calorimetry measurements using a low-cost fiber-optic probe, Appl. Spectrosc. 51 (1997) 1410–1414.
[18] J.T. Koberstein, T.P. Russell, Simultaneous SAXS-DSC study of multiple endothermic behavior in polyether-based polyurethane block copolymers, Macromolecules 19 (1986) 714–720.
[19] O.R. Dumitrescu, C. Doyle, G.F. Fernando, 30th Annual Conference, North American Thermal Analysis Society, Pittsburgh, USA, September 23–25, 2002.
[20] B. Degamber, D. Winter, J. Tetlow, M. Teagle, G.F. Fernando, Simultaneous DSC/FTIRS/TMA, J. Mater. Sci. Technol. 15 (2004) L5–L10.
[21] B. Degamber, G.F. Fernando, Fibre optic dilato-spectroscopic sensor: simultaneous thermal, spectral, and physical analyses of materials, Smart Mater. Struct. 15 (2006) 1054–1062.
[22] P.A. Crosby, G.R. Powell, G.F. Fernando, R.C. Spooncer, C.M. France, D.N.J. Waters, In situ cure monitoring of epoxy resins using optical fibre sensors, Smart Mater. Struct. 5 (1996) 415–428.
[23] I.D. Maxwell, R.A. Pethrick, Low-temperature rearrangement of amine cured epoxy-resins, Polym. Degrad. Stab. 5 (1983) 275–301.
[24] V. Strehmel, T. Scherzer, Structural investigation of epoxy-amine networks by mid-infrared and near-infrared spectroscopy, Eur. Polym. J. 30 (1994) 361–368.
[25] J. Mijovic, S. Andjelic, A study of reaction-kinetics by near-infrared spectroscopy. 1. Comprehensive analysis of a model epoxy/amine system Macromolecules 28 (1995) 2787–2796.
[26] J. Mijovic, S. Andjelic, J.M. Kenny, In situ real-time monitoring of epoxy/amine kinetics by remote near infrared spectroscopy, Polym. Adv. Technol. 7 (1996) 1–16.
[27] B. Degamber, G.F. Fernando, Fiber optic sensors for noncontact process monitoring in a microwave environment, J. Appl. Polym. Sci. 89 (2003) 3868–3873.
[28] N.A. St John, G.A. George, Cure kinetics and mechanisms of a tetraglycidyl-4,4′-diaminodiphenylmethane diaminodiphenylsulphone epoxy-resin using near IR spectroscopy, Polymer 33 (1992) 2679–2688.
[29] B.G. Min, Z.H. Stachurski, J.H. Hodgkin, G.R. Heath, Quantitative-analysis of the cure reaction of DGEBA DDS epoxy-resins without and with thermoplastic polysulfone modifier using near-infrared spectroscopy, Polymer 34 (1993) 3620–3627.
[30] A. Yoursefi, P.G. Lafleur, R. Gauvin, Kinetic studies of thermoset cure reactions: a review, Polym. Compos. 18 (1997) 157–168.
[31] C.W. Wise, W.D. Cook, A.A. Goodwin, Chemico-diffusion kinetics of model epoxy-amine resins, Polymer 38 (1997) 3251–3261.
[32] S. Sourour, M.R. Kamal, Differential scanning calorimetry of epoxy cure – isothermal cure kinetics, Thermochim. Acta 14 (1976) 41–59.
[33] S. PazAbuin, A. LopezQuintela, M. Varela, M. PazosPellin, P. Prendes, Polymer 38 (12) (1997) 3117–3120.